JOURNAL OF GUIDANCE, CONTROL, AND DYNAMICS
Vol. 39, No. 4, April 2016

Engineering Notes

Spherical Magnetic Dipole Actuator for Spacecraft Attitude Control

Joshua Chabot* and Hanspeter Schaub†
University of Colorado, Boulder, Colorado 80303

DOI: 10.2514/1.G001471

Downloaded by UNIVERSITY OF COLORADO BOULDER on June 23, 2016 | http://arc.aiaa.org | DOI: 10.2514/1.G001471

I. Introduction

THE concept of a spherical attitude actuator (also known as a reaction sphere) is similar to that of a reaction wheel; by accelerating a mass about an axis, a reaction torque is imparted on the spacecraft. With a spherical actuator, however, that axis of rotation can be arbitrary. Having a single actuator provide full attitude control is appealing because it has the potential to reduce attitude control system (ACS) mass, volume, and power requirements, all of which impact the cost of a mission. Spherical actuators also have the potential to reduce vibrational noise in a spacecraft and to increase the ACS lifespan, both of which stem from the noncontact nature of the device.

In essence, spherical actuators are three-dimensional extensions of conventional electric motors, and as with conventional electric motors, spherical actuator designs fall under two general categories: synchronous and asynchronous. Asynchronous motors use a changing magnetic field to induce a current in a nonmagnetic rotor. In turn, the induced current interacts with the changing magnetic field to produce a torque. Synchronous motors, on the other hand, rely on the coordinated interaction between permanent magnets and electromagnets to produce torque.

Chételat [1] and Rossini et al. [2] study a synchronous design that consists of a rotor with eight equally distributed permanent magnets and a stator with 20 coils. Analytical force and torque models for this actuator are developed and confirmed through finite element modeling [3] and experimental investigations [4–6]. Also, their research examines optimal stator sensor placement [3], rotor design optimization [7], back-emf modeling [2], and eddy current losses [8,9].

Instead of a multipole magnet, the design proposed here relies on a spherical dipole magnet as the rotor, as illustrated in Fig. 1. This is advantageous because dipole magnets are inexpensive, readily available, and produced from a homogeneous substrate. However, unlike with an eight-pole rotor whose magnetic field is spherically symmetric, a dipole rotor cannot provide an arbitrary torque at an instant in time because of the axisymmetry of its magnetic field. At first, this appears to be a major design flaw. However, simulations and analogous systems indicate that control is possible from such a device. In the end, the spherical dipole actuator could provide the mechanical simplicity of an asynchronous actuator with the efficiency of a synchronous device.

Received 13 May 2015; revision received 7 July 2015; accepted for publication 15 December 2015; published online 14 March 2016. Copyright © 2015 by the American Institute of Aeronautics and Astronautics, Inc. All rights reserved. Copies of this paper may be made for personal and internal use, on condition that the copier pay the per-copy fee to the Copyright Clearance Center (CCC). All requests for copying and permission to reprint should be submitted to CCC at www.copyright.com; employ the ISSN 0731-5090 (print) or 1533-3884 (online) to initiate your request.

*Master's Student, Department of Aerospace Engineering Sciences. Member AIAA.

†Professor, Department of Aerospace Engineering Sciences. Member AIAA.

II. Spherical Actuator Model

The development of the force and torque model for the proposed spherical actuator begins by examining the interaction between the rotor and an individual coil. Multiple coordinate frames are defined, as shown in Fig. 2, where $\mathcal{B}$ is a spacecraft body-fixed frame, $\mathcal{R}$ is a frame fixed to the dipole rotor and aligned with its axis of magnetization, and $\mathcal{C}_k$ is the kth coil-fixed frame aligned with the axis of the kth coil.

To find the force and torque on an individual coil caused by the magnetic field of the rotor, the Lorentz force law is first simplified by assuming there are no external electric fields present in the system:

$$\mathrm{d}\boldsymbol{F}_k = (\rho\boldsymbol{E} + \boldsymbol{J}\times\boldsymbol{B})\mathrm{d}V = (\boldsymbol{J}\times\boldsymbol{B})\mathrm{d}V \tag{1}$$

where $\mathrm{d}\boldsymbol{F}_k$ is the differential force on the coil current density $\boldsymbol{J}$ caused by the external magnetic field $\boldsymbol{B}$. Equation (1) is modified into a torque expression by taking the cross product between the position vector and the differential force element:

$$\mathrm{d}\boldsymbol{T}_k = \boldsymbol{R}\times\mathrm{d}\boldsymbol{F}_k = \boldsymbol{R}\times(\boldsymbol{J}\times\boldsymbol{B})\mathrm{d}V \tag{2}$$

Next, integrating Eqs. (1) and (2) over the volume of the coil yields the total force and torque acting on the coil:

$$\boldsymbol{F}_k = \int_V \boldsymbol{J}\times\boldsymbol{B}\,\mathrm{d}V \tag{3a}$$

$$\boldsymbol{T}_k = \int_V \boldsymbol{R}\times\boldsymbol{J}\times\boldsymbol{B}\,\mathrm{d}V \tag{3b}$$

These volume integrals can then be expanded into a useful form using spherical components, producing

$$\boldsymbol{F}_k = \int_{R_a}^{R_b}\int_{\theta_a}^{\theta_b}\int_{-\pi}^{\pi} \boldsymbol{J}\times\boldsymbol{B}\; R^2\,\sin\theta\,\mathrm{d}\phi\,\mathrm{d}\theta\,\mathrm{d}R \tag{4a}$$

$$\boldsymbol{T}_k = \int_{R_a}^{R_b}\int_{\theta_a}^{\theta_b}\int_{-\pi}^{\pi} \boldsymbol{R}\times\boldsymbol{J}\times\boldsymbol{B}\; R^2\,\sin\theta\,\mathrm{d}\phi\,\mathrm{d}\theta\,\mathrm{d}R \tag{4b}$$

As shown in Fig. 3, parameterization with spherical components is convenient because the coil is a section of a sphere delimited by its inner and outer radii, R_a and R_b, its minor and major central angles, θ_a and θ_b, and its angle of revolution, ϕ.

At this point in the development, it is useful to assign coordinate frames to the vectors. Because force and torque on a single coil are being examined, it is beneficial to express Eq. (4) in a local coil frame:

$${}^{\mathcal{C}_k}\boldsymbol{F}_k = \int_{R_a}^{R_b}\int_{\theta_a}^{\theta_b}\int_{-\pi}^{\pi} {}^{\mathcal{C}_k}\boldsymbol{J}\times{}^{\mathcal{C}_k}\boldsymbol{B}\; R^2\,\sin\theta\,\mathrm{d}\phi\,\mathrm{d}\theta\,\mathrm{d}R \tag{5a}$$

$${}^{\mathcal{C}_k}\boldsymbol{T}_k = \int_{R_a}^{R_b}\int_{\theta_a}^{\theta_b}\int_{-\pi}^{\pi} {}^{\mathcal{C}_k}\boldsymbol{R}\times{}^{\mathcal{C}_k}\boldsymbol{J}\times{}^{\mathcal{C}_k}\boldsymbol{B}\; R^2\,\sin\theta\,\mathrm{d}\phi\,\mathrm{d}\theta\,\mathrm{d}R \tag{5b}$$

where the position vector to a differential element in the coil frame is

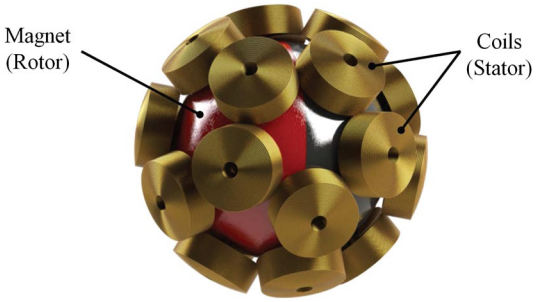

Fig. 1 Spherical dipole actuator with 20 coils.

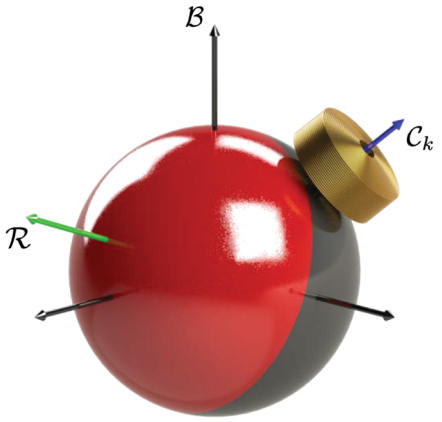

Fig. 2 Definition of spherical actuator coordinate frames.

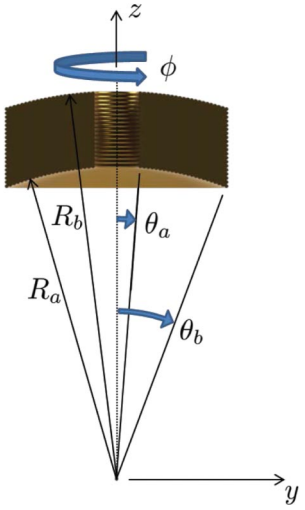

Fig. 3 Coil coordinate frame.

$$^{\mathcal{C}_k}\boldsymbol{R} = \begin{pmatrix} R\sin\theta\cos\phi \\ R\sin\theta\sin\phi \\ R\cos\theta \end{pmatrix} \tag{6}$$

and the current density vector is

$$^{\mathcal{C}_k}\boldsymbol{J} = \frac{i_k N}{A}\begin{pmatrix} -\sin\phi \\ \cos\phi \\ 0 \end{pmatrix} = \frac{2i_k N}{(R_b^2 - R_a^2)(\theta_b - \theta_a)}\begin{pmatrix} -\sin\phi \\ \cos\phi \\ 0 \end{pmatrix} \tag{7}$$

In Eq. (7), i_k denotes the kth coil current, N is the number of turns in the coil, and A is the cross-sectional area of the coil. Additionally, the magnetic field of the dipole rotor is given by

$$^{\mathcal{C}_k}\boldsymbol{B} = \frac{\mu_0}{4\pi}\left(\frac{3^{\mathcal{C}_k}\boldsymbol{\rho}(^{\mathcal{C}_k}\boldsymbol{m}\cdot{}^{\mathcal{C}_k}\boldsymbol{\rho})}{\rho^5} - \frac{^{\mathcal{C}_k}\boldsymbol{m}}{\rho^3}\right) \tag{8}$$

where $\boldsymbol{\rho}$ is the relative position between a differential coil element and the center of the rotor. Finally, to get the overall force and torque produced by the spherical actuator given an arbitrary configuration of coils, the forces and torques from each of the coils must be described in the body frame and summed together:

$$^{\mathcal{B}}\boldsymbol{f} = \sum_{k=1}^{n}[\mathcal{BC}_k]^{\mathcal{C}_k}\boldsymbol{F}_k = [\mathrm{K}_F]\boldsymbol{i} \tag{9a}$$

$$^{\mathcal{B}}\tau = \sum_{k=1}^{n}[\mathcal{BC}_k]^{\mathcal{C}_k}\boldsymbol{T}_k = [\mathrm{K}_T]\boldsymbol{i} \tag{9b}$$

where n is the number of coils in the system, $[\mathcal{BC}_k]$ transforms from the $\mathcal{C}_k$ frame to the $\mathcal{B}$ frame, $[K_F]$ and $[K_T]$ are the $3\times n$ force and torque characteristic matrices, and $\boldsymbol{i}$ is the $n\times 1$ coil current vector [4]. As it stands now, the integrals in Eq. (5) cannot be solved explicitly and must instead be integrated numerically. However, if the rotor is close to the center of the stator ($\boldsymbol{\rho}\approx\boldsymbol{R}$), analytical solutions to the volume integrals can be found allowing for real-time implementation aboard a spacecraft.

A useful measure of an actuator's performance is its power consumption. Rossini et al. develop the following spherical actuator power equation that is analogous to that of a conventional dc motor [2]:

$$P = \boldsymbol{V}^T\boldsymbol{i} = \mathrm{R}\boldsymbol{i}^T\boldsymbol{i} + \frac{1}{2}\frac{d}{dt}\left(\boldsymbol{i}^T[L]\boldsymbol{i}\right) + \boldsymbol{\omega}_{\mathcal{B}/\mathcal{N}}[K_T]\boldsymbol{i} \tag{10}$$

Note that, in this equation, the induction term $[L]$ is a matrix that describes the mutual and self-induction of the coil array and that the motor constant $[K_T]$ is the matrix found in Eq. (9b). For the simulations presented here, the induction term is assumed to be negligible compared to the other terms and is therefore ignored to simplify the power model.

III. Spacecraft Equations of Motion

The total angular momentum for a spacecraft with a spherical actuator is given by

$$\boldsymbol{H} = \boldsymbol{H}_B + \boldsymbol{H}_R \tag{11}$$

where $\boldsymbol{H}_B$ and $\boldsymbol{H}_R$ are the momenta of the spacecraft body and the spherical actuator, respectively. The time rate of change of angular momentum about the system's center of mass is equivalent to the net external torque on the system:

$$\dot{\boldsymbol{H}} = \dot{\boldsymbol{H}}_B + \dot{\boldsymbol{H}}_R = \boldsymbol{L} \tag{12}$$

Expanding these inertial derivatives and rearranging yields

$$[I_B]\dot{\boldsymbol{\omega}}_{\mathcal{B}/\mathcal{N}} + \boldsymbol{\omega}_{\mathcal{B}/\mathcal{N}}\times[I_B]\boldsymbol{\omega}_{\mathcal{B}/\mathcal{N}} = \boldsymbol{\tau} + \boldsymbol{L} \tag{13}$$

where $\boldsymbol{\omega}_{\mathcal{B}/\mathcal{N}}$ is the spacecraft body rate vector with respect to an inertial frame, and $[I_B]$ is the spacecraft inertia tensor. As can be seen from Eq. (13), the torque produced by a spherical actuator is simply an external torque on the spacecraft. A more detailed derivation of Eq. (13) can be found in Chabot and Schaub [10].

Along with the spacecraft dynamics equations, an attitude parameterization is necessary. Modified Rodrigues parameters (MRPs) are chosen, and therefore the MRP attitude kinematic differential equation is given by

$$\dot{\boldsymbol{\sigma}} = \frac{1}{4}[(1-\boldsymbol{\sigma}^T\boldsymbol{\sigma})[I_{3\times3}] + 2\tilde{\boldsymbol{\sigma}} + 2\boldsymbol{\sigma}\boldsymbol{\sigma}^T]\boldsymbol{\omega} \tag{14}$$

where $\boldsymbol{\sigma}$ is the MRP attitude vector. To avoid the MRP singularity, the norm of $\boldsymbol{\sigma}$ is kept less than or equal to unity by switching to the MRP shadow set when necessary. This also ensures that the shorter attitude control trajectory will be chosen [11].

Downloaded by UNIVERSITY OF COLORADO BOULDER on June 23, 2016 | http://arc.aiaa.org | DOI: 10.2514/1.G001471

Table 1 Simulation parameters

Parameter	Value	Parameter	Value
Number of coils	20	Spacecraft inertia $[I]$	diag ([0.02 0.03 0.08]) kg · m^2
Windings per coil, N	334	Actuator position $\boldsymbol{D}$	[10 10 10]^T cm
Inner coil radius R_a	20 mm	P gain	0.008 N · m
Outer coil radius R_b	24 mm	$[D]$ gain	[0.01 0.01 0.03] N · m · s
Inner coil angle θ_a	2.5 deg	K_P gain	550 s^{-2}
Outer coil angle θ_b	20 deg	K_D gain	110 s^{-1}
Rotor radius	18 mm	Magnetic moment $\boldsymbol{m}$	25.66 N · m/T
Rotor mass	182 g		

The following feedback control law is used to stabilize the spacecraft relative to the attitude origin:

$$\boldsymbol{\tau} = -P\boldsymbol{\sigma} - [D]\boldsymbol{\omega} \tag{15}$$

where P is a positive scalar, and $[D]$ is a positive-definite matrix. This attitude regulation control law is globally asymptotically stabilizing if no unmodeled torques are present, which is the case for all simulations presented here [11,12]. Note that the following developments are not tied to this particular choice of attitude control law in Eq. (15). Rather, this proportional–derivative (PD) regulation control can be substituted with any desired attitude control torque expression, including a reference tracking control. Of interest is how the desired control torque $\boldsymbol{\tau}$ is generated through the rotors and coils.

The relationships between coil current and actuator force and torque that are established in Eq. (9) can now be used to calculate the necessary coil current vector, given a desired spacecraft torque command. For the case where only a single spherical actuator is used,

$$\begin{bmatrix} K_T \\ K_F \end{bmatrix} \boldsymbol{i} = \begin{bmatrix} \boldsymbol{\tau} \\ \boldsymbol{f} \end{bmatrix} \tag{16}$$

relates coil currents to forces and torques. Here, the rotor position control force $\boldsymbol{f}$ is given by a closed-loop feedback control law. A simple PD controller is chosen to provide rotor position control:

$$\boldsymbol{f} = -K_P\boldsymbol{r} - K_D\dot{\boldsymbol{r}} \tag{17}$$

where K_P and K_D are positive scalar gains, $\boldsymbol{r}$ is the rotor position error, and $\dot{\boldsymbol{r}}$ is the rotor velocity error. The position error is given by

$$\boldsymbol{r} = \boldsymbol{D}' - \boldsymbol{D} \tag{18}$$

where $\boldsymbol{D}'$ is the actual position of the rotor with respect to the spacecraft center of mass, and $\boldsymbol{D}$ is the position of the center of the stator with respect to the center of mass, which is constant as seen from the body frame.

The coil current vector in Eq. (16) can then be found by applying a Moore–Penrose pseudoinverse:

$$\boldsymbol{i} = \begin{bmatrix} K_T \\ K_F \end{bmatrix}^+ \begin{bmatrix} \boldsymbol{\tau} \\ \boldsymbol{f} \end{bmatrix} \tag{19}$$

Because of the axisymmetry of the dipole rotor, $[K_T]$ is rank 2, and therefore there is a null space of torques that cannot be produced by the single actuator at an instant in time. In instances where a torque cannot be produced, the pseudoinverse finds the least-squares solution to this rank-deficient problem. The characteristic force matrix $[K_F]$, however, is always full rank and can therefore provide the desired position control force.

IV. Numerical Simulations

For all simulations presented here, the parameters in Table 1 are used. The rotor is assumed to be solid and uniformly magnetized and to have no spin rate at the beginning of the maneuver. These design parameters are chosen such that the inertia about the rotor spin axis is equivalent to the spin axis inertia of the reaction wheel system discussed in Sec. V. Additionally, all simulations assume that the rotor is close to the center of the stator and therefore use the analytical force and torque expressions, drastically reducing simulation time.

Despite the axisymmetry of the dipole field, the proposed spherical actuator successfully detumbles and points a spacecraft, as illustrated by Figs. 4a and 4b. The peak power consumption for the device occurs at the beginning of the maneuver and is 56.9 mW. The power consumption plot also illustrates how the rotor position control effort is negligible compared to the torque control effort. Additionally, simulations show that even for scenarios where the spherical actuator is placed far from the center of mass and the spacecraft tumbles with a large initial body rate, the rotor position control is successful and requires minimal effort [10].

Although it is not rigorously proven here, attitude controllability arguments can likely be made for the single spherical dipole actuator. Only a subspace of control torques are producible at an instant in time; however, this subspace depends on the orientation of the rotor and is therefore time-varying. Attitude control of a spacecraft with three independent magnetorquers is a close analog to the spherical dipole actuator and is controllable despite being underactuated, as is discussed in [13–18] and proven in [19]. With Earth's magnetic field modeled as a dipole, the torque capability of the three magnetorquers does not span three-dimensional space at an instant in time. However, the controllable subspace of this system varies with the orbit of the spacecraft, resulting in controllability.

Both magnetic attitude control and the spherical actuator do suffer from a singularity, though. In the orbiting spacecraft attitude control scenario, controllability is lost if the spacecraft is in an equatorial orbit. Similarly with the spherical actuator, a torque cannot be produced about the rotor's magnetic moment vector. This situation is highly unlikely, however, because this alignment of the magnetic moment vector with the commanded torque would be instantaneous thanks to the relative motion between the spacecraft body and rotor. Simulations confirm this and show that even in cases where the actuator is close to a singular configuration, control is achieved without loss of performance [10].

V. Comparison to Reaction Wheel System

Reaction wheel control systems are commonly found on spacecraft, and because of this, they serve as a good benchmark for judging the performance of the spherical actuator. The motor torque constant K is often used to compare motor capabilities, such as power consumption and efficiency. However, with the spherical actuator, $[K_T]$ is time-varying, making this difficult. As such, a commercially available cluster of three reaction wheels for small satellites sold by Blue Canyon Technologies (BCT)[‡] is simulated for comparison and is shown in Fig. 5.

Table 2 provides a side-by-side comparison of some of the key parameters from the spherical actuator and reaction wheel simulations, where the same attitude maneuver is performed. As can be seen, the mass for the spherical actuator and reaction wheel cluster are similar. However, the spherical actuator mass only accounts for the mass of the rotor and the coils and does not account for electronics

[‡]Data available online at http://bluecanyontech.com/ [retrieved 10 February 2015].

Downloaded by UNIVERSITY OF COLORADO BOULDER on June 23, 2016 | http://arc.aiaa.org | DOI: 10.2514/1.G001471

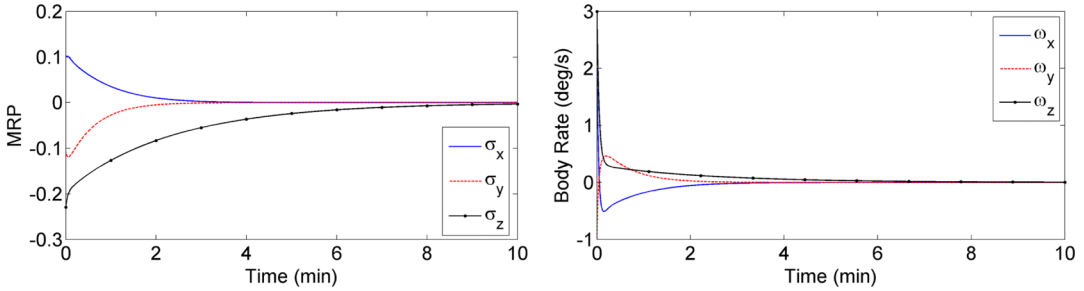

a) Spacecraft attitude error b) Spacecraft body rate error

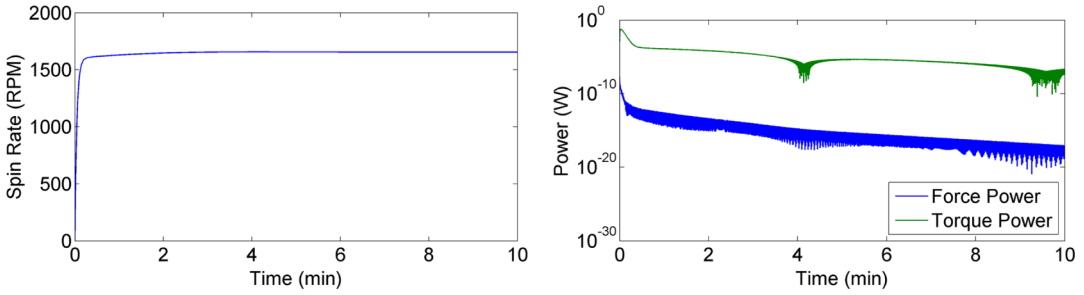

c) Rotor spin rate d) Actuator power consumption

Fig. 4 Single actuator attitude control maneuver.

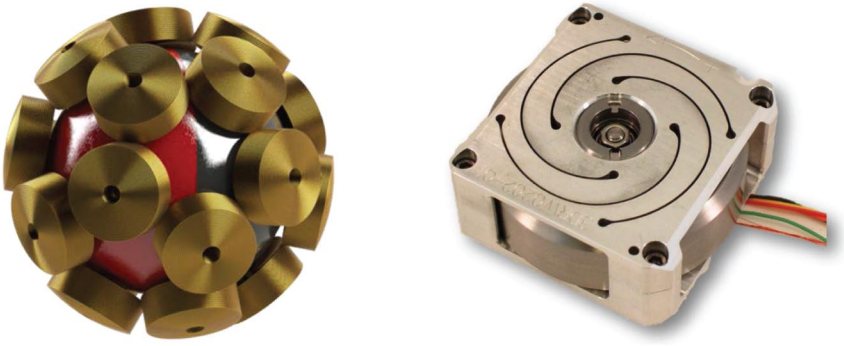

a) Spherical dipole actuator b) Micro reaction wheel from BCT

Fig. 5 ACS comparison.

and support structures. The volumes for the two systems vary significantly, with the spherical actuator filling a volume almost half that of the reaction wheel cluster. Note that the spherical actuator volume is the spherical volume determined by the outer radius of the coils, and the reaction wheel cluster volume was determined by summing the individual volumes of the three reaction wheels as determined by the dimensions provided by BCT. Furthermore, there are substantial power and energy savings with the spherical actuator.

Although the motor torque constant and electrical resistance for the commercial reaction wheel system are empirical values, which is not the case for the spherical actuator, the dynamics model for the reaction wheels does not take into account frictional and viscous losses. Of course, there are many design concerns that would affect the geometry and performance of the spherical actuator that are not included here. However, these results do indicate potential savings and benefits associated with the spherical magnetic dipole actuator.

Table 2 ACS parameter comparison

Parameter	Spherical actuator	Reaction wheel cluster
Inertia, g · cm^2	240	240
Mass, g	311	345
Volume, cm^3	57.9	99.85
Peak power, mW	56.9	217
Maneuver energy, mJ	309	678

VI. Conclusions

A spherical actuator for spacecraft attitude control has been presented here that relies on a simple dipole magnet to exchange momentum with the spacecraft. The equations of motion for this system, along with an analytical force and torque model, were derived and numerically simulated, indicating that the proposed actuator can provide attitude control. Further research into this form of underactuated control is necessary to fully understand how effective a single actuator can be. However, simulations conducted thus far and analogous underactuated systems indicate that control arguments can be made. Finally, the spherical actuator was compared against a cluster of three reaction wheels and was found to provide mass, volume, and power savings.

References

[1] Chételat, O., "Torquer Apparatus," U.S. Patent 8,164,294, filed 24 April 2012.

[2] Rossini, L., Onillon, E., Chetelat, O., and Perriard, Y., "Back-EMF and Rotor Angular Velocity Estimation for a Reaction Sphere Actuator," *2014 IEEE/ASME International Conference on Advanced Intelligent Mechatronics (AIM)*, IEEE Publ., Piscataway, NJ, 2014, pp. 334–339. doi:10.1109/AIM.2014.6878101

[3] Rossini, L., Onillon, E., Chetelat, O., and Perriard, Y., "An Optimal Sensor Placement Strategy for Force and Torque Analytical Models of a Reaction Sphere Actuator for Satellite Attitude Control," *Proceedings of the 2012 XXth International Conference on Electrical Machines*

Downloaded by UNIVERSITY OF COLORADO BOULDER on June 23, 2016 | http://arc.aiaa.org | DOI: 10.2514/1.G001471

(ICEM), IEEE Publ., Piscataway, NJ, 2012, pp. 2545–2551. doi:10.1109/ICElMach.2012.6350243

[4] Rossini, L., Chetelat, O., Onillon, E., and Perriard, Y., "Analytical and Experimental Investigation on the Force and Torque of a Reaction Sphere for Satellite Attitude Control," *2011 IEEE/ASME International Conference on Advanced Intelligent Mechatronics (AIM 2011)*, IEEE Publ., Piscataway, NJ, 2011, pp. 487–492. doi:10.1109/AIM.2011.6026980

[5] Rossini, L., Chetelat, O., Onillon, E., and Perriard, Y., "An Open-Loop Control Strategy of a Reaction Sphere for Satellite Attitude Control," *2011 International Conference on Electrical Machines and Systems*, IEEE Publ., Piscataway, NJ, 2011, pp. 3652–3657. doi:10.1109/ICEMS.2011.6073912

[6] Rossini, L., Chetelat, O., Onillon, E., and Perriard, Y., "Force and Torque Analytical Models of a Reaction Sphere Actuator Based on Spherical Harmonic Rotation and Decomposition," *IEEE/ASME Transactions on Mechatronics*, Vol. 18, No. 3, 2013, pp. 1006–1018. doi:10.1109/TMECH.2012.2195501

[7] Rossini, L., Mingard, S., Boletis, A., Forzani, E., Onillon, E., and Perriard, Y., "Rotor Design Optimization for a Reaction Sphere Actuator," *IEEE Transactions on Industry Applications*, Vol. 50, No. 3, 2014, pp. 1706–1716. doi:10.1109/TIA.2013.2282660

[8] Strumik, M., Wawrzaszek, R., Banaszkiewicz, M., Seweryn, K., Sidz, M., Onillon, E., and Rossini, L., "Analytical Model of Eddy Currents in a Reaction Sphere Actuator," *IEEE Transactions on Magnetics*, Vol. 50, No. 6, Jan. 2014, Paper 4004607. doi:10.1109/TMAG.2014.2298215

[9] Wawrzaszek, R., Strumik, M., Seweryn, K., Sidz, M., Banaszkiewicz, M., Rossini, L., and Onillon, E., "Electromagnetic Compatibility Problems of ELSA—Novel Component for Spacecraft Attitude Control System Based on Concept of Spherical Actuator," *2013 18th International Conference on Methods & Models in Automation & Robotics (MMAR)*, IEEE Publ., Piscataway, NJ, 2013, pp. 572–527. doi:10.1109/MMAR.2013.6669974

[10] Chabot, J., and Schaub, H., "A Spherical Magnetic Dipole Actuator for Spacecraft Attitude Control," Master's Thesis, Aerospace Engineering Sciences Dept., Univ. of Colorado, Boulder, CO, 2015.

[11] Schaub, H., and Junkins, J. L., *Analytical Mechanics of Space Systems*, 3rd ed., AIAA Education Series, AIAA, Reston, VA, 2014, pp. 405–416. doi:10.2514/4.102400

[12] Tsiotras, P., "A Passivity Approach to Attitude Stabilization Using Nonredundant Kinematic Parameterizations," *Proceedings of the 34th IEEE Conference on Decision and Control*, Vol. 1, IEEE Publ., Piscataway, NJ, 1995, pp. 515–520. doi:10.1109/CDC.1995.478944

[13] Lovera, M., De Marchi, E., and Bittanti, S., "Periodic Attitude Control Techniques for Small Satellites with Magnetic Actuators," *IEEE Transactions on Control Systems Technology*, Vol. 10, No. 1, 2002, pp. 90–95. doi:10.1109/87.974341

[14] Psiaki, M., "Magnetic Torquer Attitude Control via Asymptotic Periodic Linear Quadratic Regulation," *Journal of Guidance, Control, and Dynamics*, Vol. 24, No. 2, 2001, pp. 386–94. doi:10.2514/2.4723

[15] Wisniewski, R., "Linear Time-Varying Approach to Satellite Attitude Control Using only Electromagnetic Actuation," *Journal of Guidance, Control, and Dynamics*, Vol. 23, No. 4, 2000, pp. 640–647. doi:10.2514/2.4609

[16] Silani, E., and Lovera, M., "Magnetic Spacecraft Attitude Control: A Survey and Some New Results," *Control Engineering Practice*, Vol. 13, No. 3, 2005, pp. 357–371. doi:10.1016/j.conengprac.2003.12.017

[17] Astolfi, A., and Lovera, M., "Global Spacecraft Attitude Control Using Magnetic Actuators," *Proceedings of the 2002 American Control Conference*, Vol. 2, IEEE Publ., Piscataway, NJ, 2002, pp. 1331–1335. doi: 10.1109/ACC.2002.1023205.

[18] Pittelkau, M., "Optimal Periodic Control for Spacecraft Pointing and Attitude Determination," *Journal of Guidance, Control, and Dynamics*, Vol. 16, No. 6, 1993, pp. 1078–84. doi:10.2514/3.21130

[19] Bhat, S. P., "Controllability of Nonlinear Time-Varying Systems: Applications to Spacecraft Attitude Control Using Magnetic Actuation," *IEEE Transactions on Automatic Control*, Vol. 50, No. 11, 2005, pp. 1725–1735. doi:10.1109/TAC.2005.858686

Downloaded by UNIVERSITY OF COLORADO BOULDER on June 23, 2016 | http://arc.aiaa.org | DOI: 10.2514/1.G001471